HEAT TRANSFER PERFORMANCE OF FILM CONDENSATION CREATED BY FORCED FLOW

Mohamed El-Sayed Mosaad

Faculty of Technological studies of PAAET, Kuwait, **mosaad77@hotmail.com**

In this work, condensate film on a vertical wall cooled on the external side by forced flow is analysed as a conjugate heat transfer problem. The treated case is that the condensate film and forced flow boundary layer are in a parallel-flow arrangement. The mass, momentum and energy boundary layer equations of the condensate film and forced flow are set in a dimensionless form to generalize the model. The parameters affecting the thermal communication between the condensate film and the forced flow are defined from the analysis. These parameters explain the relative impact of the three involved thermal resistances of solid wall, forced convection and film condensation on the local and mean Nusselt number. The study shows that the Nusselt number predicted by the present conjugate model is different from that predicted by a Nusselt-type model.

Keywords: *Film condensation, Forced convection, Conjugate heat transfer*.

1. Introduction

Many film condensation studies have been done since the original work of Nusselt [1]. The objective was to modify Nusselt model by including the effects of some neglected factors, for example vapour superheat [2], vapor shear [3], film convection [4], flow regimes [5], and surface shape [6, 7] among other factors. In these modified Nusselt-model studies, either a constant temperature or heat flux was assumed at the wall side facing the condensate film without considering the effect of the fluid cooling the back wall side. In fact, this cooling fluid can cause a considerable variation in the wall temperature or/and heat flux. Consequently, the assumption of a constant wall temperature or heat flux commonly applied in a Nusselt-type model is considered inappropriate. Therefore, some recent studies have treated the film condensation as a conjugate heat transfer problem to inspect the impact of the back-cooling fluid. In addition, the assumption of a constant wall temperature or heat flux is not made in the conjugate analysis, but these wall thermal conditions are discovered from the solution.

Some recent authors studied the conjugate problem of film condensation and free convection. Poulikakos [8] did the first study for a solid vertical wall of zero thermal resistance by adopting the Nusselt theory for analyzing the condensate film, and using the Osceen technique for solving the free convection mode. Later, Char and Lin [9] employed the Spline method to treat the same problem for a vertical wall embedded in a porous fluid medium. Later on, Mosaad [10, 11] employed the integral method to analyze the film condensation and the analytical Osceen tool to solve the natural convection boundary layer for a vertical wall of negligible [10] or considerable thermal resistance [11]. He found that the conjugate results are different from that of a classical Nusselt-type model.

Regarding the topic of coupled film condensation and forced convection, Patankar and Sparrow [12] did the first numerical study by using a similarity technique to treat film condensation outside a vertical tube cooled by internal forced flow. They simplified their model by considering only the thermal interaction between the condensate film and wall conduction and neglecting the effect of the internal flow. Later, Faghri and Sparrow [13] treated numerically the same problem of Patankar and Sparrow, however for a tube

of negligible wall resistance. Consequently, they modeled only the thermal coupling between the condensate film and the internal fluid flow. Kose [14] treated analytically and numerically film condensation inside a vertical tube cooled by external forced flow, and proved numerically that the ratio of axial to radial heat flux is less than 0.05%. Based on this outcome, the axial wall conduction was neglected in his analytical solution. Chen and Chang [15] applied the non-similarity method to solve numerically conjugated film condensation and forced convection in counter-flow on the opposite sides of a vertical wall. They neglected the axial wall conduction and proved that the wall resistance has a remarkable effect on the solution. Bautista et al. [16] employed a perturbation method to study film condensation outside a vertical two-plate channel cooled internally by a forced flow. They concluded that non-conjugate Nusselt-type models are not suitable to be used for predicting exactly the necessary heat transfer surface area of a vapour condenser. Later, Luna and Méndez [17], who solved the same problem for a porous-medium channel, stated like results.

The above review indicates that only limited-number studies were conducted on the thermal coupling between film condensation and forced flow. Therefore, more studies are still needed to achieve better understanding of this conjugate heat transfer process, as well as to explain the effect of the solid wall resistance in some details. Therefore, in the present work, the problem of coupled condensate film and forced convection in a parallel-flow arrangement on vertical wall sides is treated analytically. The main benefit of like an analytical treatment is that the effect of the dimensionless factors controlling the thermal communication process becomes more understandable than in a numerical model. As a brief description of the present model described next, the forced convection boundary layer is analyzed by an integral technique, while the treatment of the condensate film is based on the boundary layer theory and Nusselt simplifications. The two analysis results are matched at the wall sides by applying the interfacial thermal conditions to give the final solution. The analysis is done in a dimensionless framework to generalize the model.

2. Analysis

A sketch of the model is plotted in Fig. 1. The plot shows that a pure stagnant vapour of saturation temperature T_s condenses on the side of a solid vertical wall (length H and thickness w) by the impact of cold fluid flowing with free-stream velocity $u_{c\infty}$ on the opposite wall side. The cooling fluid is at a free-stream temperature $T_{c\infty}$, much less than the vapour saturation temperature T_s. The wall ends are thermally insulated. The investigated case is that the generated condensate film and convection boundary layer are in a parallel-flow arrangement.

Because of the mathematical complexity encountered in solving analytically such a conjugate heat transfer problem, few simplifications are made to simplify the analysis. It is considered that the flow in both condensate film and convection boundary layer is steady, laminar and of a negligible viscous dissipation. It is also assumed that the pressure gradient outside the two layers is zero, and the two fluids are of constant thermal properties and Prandtl number $Pr \geq 1$. For simplicity in the mathematical modelling, the same temperature symbol T is taken for both fluid and solid. In addition, the subscripts "c", "f" and "w" are introduced to designate the cooling fluid, the condensate film and the solid wall, respectively.

2.1. Condensate Film

For the above-mentioned simplifications, the equations of the mass, momentum and energy conservation in the condensate film can be expressed, respectively, by

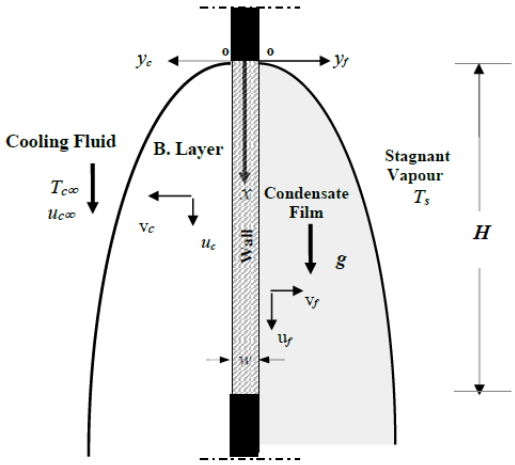

Fig. 1 Model illustration

$$\frac{\partial U_f}{\partial X} + \frac{\partial V_f}{\partial Y_f} = 0 \tag{1}$$

$$U_f \frac{\partial U_f}{\partial X} + V_f \frac{\partial U_f}{\partial Y_f} = \frac{Pr_f}{Ja}\left(\frac{\partial^2 U_f}{\partial Y_f^2} - 1\right) \tag{2}$$

$$U_f \frac{\partial \theta}{\partial X_f} + V_f \frac{\partial \theta}{\partial Y_f} = \frac{1}{Ja}\frac{\partial^2 \theta}{\partial Y_f^{\,2}} \tag{3}$$

The dimensionless variables presented above are defined:

$$\begin{gathered} Y_f = y_f/l_f,\ X = x/H,\quad U_f = u_f/(Ja\,\alpha_f H/l_f^2),\ V_f = v_f/(Ja\,\alpha_f/l_f),\ \theta = (T-T_{c\infty})/(T_s-T_{c\infty}), \\ \Delta_f = \delta_f/l_f,\ \theta_{wf} = (T_{wf}-T_{c\infty})/(T_s-T_{c\infty}),\quad Ra_f = gH^3(\rho_f-\rho_v)h_{fg}/(k_f \nu_f (T_s-T_{c\infty})),\ l_f = HRa_f^{-1/4}. \end{gathered} \tag{4}$$

Wherein, the dimensional parameters θ, Ja, Δ_f, l_f and Ra_f sign respectively to temperature, Jacob number, film thickness, film thickness scale, and film Rayleigh number.

The appropriate boundary conditions are:

$$\begin{array}{lll} Y_f = 0; & U_f = V_f = 0 & \text{and} \quad \theta = \theta_{wf}, \\ Y_f = \Delta_f; & \partial U_f/\partial Y_f = 0, & \text{and} \quad \theta = 1, \\ X = 0; & \Delta_f = 0 & \text{and} \quad \theta = 1. \end{array} \tag{5}$$

The dimensionless wall-film interface temperature θ_{wf} is assumed an arbitrary function of *x*-coordinate, which has to be defined from the solution.

For most practical fluids of $Pr_f \geq 1$ and: $10^{-3} < Ja \leq 10^{-1}$, the inertia and convection terms in the above momentum and energy equations can be neglected [10]. Hence, solving the two reduced equations for boundary conditions (5) gives the velocity and temperatures profiles by

$$U_f = 0.5 Y_f^2 \left(2\Delta_f/Y_f - 1\right), \tag{6}$$

$$\theta = \theta_{wf}(1 - Y_f/\Delta_f) + Y_f/\Delta_f \tag{7}$$

The heat balance at the condensate-vapour interface is expressed by

$$\left.\frac{d\,\theta}{\mathrm{d}Y_f}\right|_{Y_f\,=\,\Delta_f} = \left(U_f\,\frac{d\,\Delta_f}{dX} - \mathrm{V}_f\right)_{Y_f\,=\,\Delta_f} \tag{8}$$

Substituting U_f, θ from Eqs. (6) & (7) and V_f from integrating Eq. (1) into Eq. (8), this gives

$$\frac{d\,\Delta_f}{dX} = \frac{(1-\theta_{wf})}{\Delta_f^3} \tag{9}$$

The above relation is the main result of the condensate film analysis.

2.2 Forced convection

For steady, incompressible, laminar forced flow of constant properties on a vertical solid surface, the boundary layer equations of mass, momentum and energy conservation read, respectively, as

$$\frac{\partial u_c}{\partial x} + \frac{\partial \mathrm{v}_c}{\partial y_c} = 0 \tag{10a}$$

$$u_c\,\frac{\partial u_c}{\partial x} + \mathrm{v}_c\,\frac{\partial u_c}{\partial y_c} = -\frac{1}{\rho_c}\frac{dp}{dx} + \nu_c\,\frac{\partial^2 u_c}{\partial y_c^2} \tag{10b}$$

$$u_c\,\frac{\partial T}{\partial x} + \mathrm{v}_c\,\frac{\partial T}{\partial y_c} = \alpha_c\,\frac{\partial^2 T}{\partial y_c^2} \tag{10c}$$

Integrating momentum Eq. (10b) across the hydrodynamic boundary layer for zero outside pressure gradient condition gives:

$$\frac{d}{dX}\int_0^{\Delta_c} U_c(1-U_c)\,dY_c = \left.\frac{\partial U_c}{\partial Y_c}\right|_{Y_c=0}. \tag{11a}$$

So, integrating Eq. (10c) across the thermal boundary layer yields

$$\frac{d}{dX}\int_0^{\Delta_{tc}} Pr_c\,U_c\theta\,dY_c = -\left.\frac{\partial\theta}{\partial Y_c}\right|_{Y_c=0}. \tag{11b}$$

The relevant boundary conditions are:

$$\begin{aligned} &X = 0;\quad U_c = 0,\quad \theta = 0,\\ &Y_c = 0;\quad U_c = 0,\quad \partial^2 U_c/\partial Y_c^{\,2} = 0,\quad \theta = \theta_{wc},\quad \partial^2\theta/\partial Y_c^{\,2} = 0\\ &Y_c = \Delta_c;\quad U_c = 1,\quad \partial U_c/\partial Y_c = 0\ \ \&\ \ Y_c = \Delta_{tc};\quad \theta = 0,\quad \partial\theta/\partial Y_c = 0. \end{aligned} \tag{12}$$

The dimensionless variables introduced are defined as:

$$Y_c = \frac{y_c}{H}Re^{1/2},\ \Delta_c = \frac{\delta_c}{H}\,Re^{1/2},\ \Delta_{ct} = \frac{\delta_{ct}}{H}Re^{1/2},\ U_c = \frac{u_c}{u_{c\infty}}\ \&\ \theta_{wc} = \frac{T_{wc}-T_{c\infty}}{T_s-T_{c\infty}}. \tag{13}$$

The symbols Re and Pr_c refers, respectively, to Reynolds number and Prandtl number, while Δ_c and Δ_{ct} sign, respectively, to the velocity and thermal boundary layer thickness, and U_c & θ denote to the velocity and temperature, respectively. The symbol θ_{wc} is the temperature of the convection wall side, which is an unknown *x*-function found from the solution. According boundary conditions (12), the crosswise velocity and temperature profiles can be defined by:

$$U_c = 1.5\,(Y_c/\Delta_c) \;-\; 0.5(Y_c/\Delta_c)^3; \qquad 0 \le Y_c \le \Delta_c, \tag{14}$$

$$\theta = \theta_{wc}\left(1-1.5(Y_c/\Delta_{tc})+.5(Y_c/\Delta_{tc})^3\right); \qquad 0 \le Y_c \le \Delta_{tc}. \tag{15}$$

Solving Eqs. (11a) & (11b) for the two above profiles gives

$$\frac{d\Delta_{tc}}{dX} = 10\theta_{wc}/(\phi Pr_c\Delta_{tc}) - \frac{\Delta_{tc}}{\theta_{wc}}\frac{d\,\theta_{wc}}{dX}; \quad \text{for } \phi = \Delta_{tc}/\Delta_c \text{ and } \Delta_c = \sqrt{280X/13}\,). \tag{16}$$

Wherein ϕ is the thickness ratio of thermal to velocity boundary layer, which can be approximated by $\phi = 0.976\,Pr_c^{-1/3}$; for $1 \le Pr_c \le 50$ [10].

Relation (16) is considered the main result of the condensate film analysis.

Now, the next task is to combine the two main results (9) & (16). This task can be accomplished by applying the thermal interfacial conditions on both wall sides. Assuming the thickness-to-height ratio of the solid separating wall is much less than 1, wall conduction can be considered mainly in the crosswise direction. Accordingly, the transverse wall temperature profile can be expressed by

$$\theta = \theta_{wc} + \left(\theta_{wf} - \theta_{wc}\right)Y_w; \text{ for } Y_w = y_w/w \tag{17}$$

The continuity conditions of the heat flux and temperature at both wall sides can be expressed by

$$\theta_f'(X,0) = -\lambda\,\theta_c'(X,0) = \frac{\lambda}{\varepsilon_w}(\theta_{wf} - \theta_{wc}) \tag{18}$$

$\theta_f'(X,0)$ and $\theta_c'(X,0)$ are, respectively, the temperature gradients of condensate film and convection layer at the wall. The two dimensionless parameters λ and ε_w in Eq. (18) are defined by:

$$\varepsilon_w = \frac{w\,k_c}{H\,k_w}\,Re^{0.5}, \;\; \& \;\; \lambda = \frac{k_c}{k_f}\frac{Re^{0.5}}{Ra_f^{0.25}}. \tag{19}$$

The variables ε_w denotes to the ratio of solid wall resistance to forced convection resistance layer. The variables λ denotes to the ratio of condensate film resistance to forced convection resistance.

Calculating the temperature derivative terms in Eq. (18) from Eqs. (7) & (15), this gives

$$\theta_{wf} \;=\; 1 - \Delta_f/\Psi; \tag{20}$$

$$\theta_{wc} \;=\; 2\Delta_{tc}/(3\lambda\psi); \;\; \text{for} \;\; \Psi \;=\; (\Delta_f + 2\Delta_{tc}/3\lambda + \varepsilon_w/\lambda) \tag{21}$$

Relation (20) for $\Delta_f = 0$ gives $\theta_{wf} = 1$, while expression (21) for $\Delta_{tc} = 0$ gives $\theta_{wc} = 0$. This indicates that the two relations satisfy the initial conditions of $\theta_{wf} = 1$ and $\theta_{wc} = 0$ at $X = 0$ (cf., Eqs. (5) & (12)).

Inserting θ_{wf} & θ_{wc} from Eqs. (20) & (21) into Eqs. (9) & (17), this gives after separating the variables:

$$\frac{d\Delta_f}{dX} \;=\; \frac{1}{\Psi\Delta_f^2}; \tag{22}$$

$$\frac{\mathrm{d}\,\Delta_{tc}}{\mathrm{d}X} \;=\; \frac{15\Psi}{\phi Pr_c\,\Delta_{tc}(3\Psi - \Delta_{tc}/\lambda)} + \frac{3\Delta_{tc}}{2\Psi(3\Psi - \Delta_{tc}/\lambda)\,\Delta_f^2} \tag{23}$$

The local Nusselt number can be calculated from the local heat flux at the solid-film interface divided by the total temperature drop $(T_s - T_{c\infty})$. This gives

$$\frac{Nu_x}{Ra_{fx}^{0.25}} = \sqrt[4]{X}\,\theta_f'(X,0) = \frac{\sqrt[4]{X}}{\Delta_f}(1-\theta_{wf}) \tag{24a}$$

Subsequently, the mean conjugate Nusselt number is calculated by

$$\frac{Nu}{Ra_f^{0.25}} = \int_0^1 \theta_f'(X,0)dX = \int_0^1 \frac{(1-\theta_{wf})}{\Delta_f}\,dX \tag{24b}$$

Alternatively, the local and mean conjugate Nusselt numbers can be expressed in terms of the local heat flux at the solid-convection interface divided by total temperature drop $(T_s - T_{c\infty})$. This gives:

$$\frac{Nu_x}{Re_x^{0.5}\,Pr_c^{1/3}} = \frac{\sqrt{X}}{Pr_c^{1/3}}\,\theta_c'(X,0) = \frac{3\sqrt{X}}{2\Delta_{tc}\,Pr_c^{1/3}}\,\theta_{wc} \tag{25a}$$

$$\frac{Nu}{Re^{0.5}Pr_c^{1/3}} = \frac{1}{Pr_c^{1/3}}\int_0^1 \theta_c'(X,0)\,dX = \frac{1}{Pr_c^{1/3}}\int_0^1 \frac{3\theta_{wc}}{2\Delta_{tc}}\,dX \tag{25b}$$

3. Solution

3.1 Analytical solution

In this context, special analytical results are found from the general analysis derived above. For the simplified problem case of negligible wall resistance of $\varepsilon_w \to 0$, the separating wall becomes as an interfacial surface between the two fluid media, whose dimensionless temperature θ_w is function only of *X*-coordinate. For this case of $\varepsilon_w \to 0$, Eqs. (20) & (21) indicate that $\theta_{wf} \to 0 \,\&\, \theta_{wc} \to 0$, as $\lambda \to \infty$. This means that on these limits of $\varepsilon_w \to 0$ and $\lambda \to \infty$, the wall temperature assumes the free-stream temperature of the convection side of zero dimensionless value. This indicates disappearing the forced convection boundary layer. Consequently, the treated two-fluid problem reduces to the traditional one-fluid problem of film condensation on isothermal surfaces. This outcome is expected subject to the physical meaning of λ – variables defined by Eq. (19). Now, solving Eqs. (24a, b) with Eq. (9) for $\theta_{wf} \to 0$ and $\varepsilon_w \to 0$ gives

$$Nu_x \big/ Ra_{fx}^{0.25} = 0.707 \tag{27}$$

$$Nu \big/ Ra_f^{0.25} = 0.943 \tag{28}$$

The two above results are the same exact Nusselt ones of laminar film. On the other limit of $\lambda \to 0$, Eqs. (20) & (21) for $\varepsilon_w \to 0$ show that $\theta_{wf} \to 1$ and $\theta_{wc} \to 1$. This means that the wall will take the vapour saturation temperature of the condensation side of the one dimensionless value. This means collapsing the film condensation, and consequently, reducing the conjugate problem to the simple one-fluid problem of forced flow on an isothermal vertical surface. Now, solving Eqs. (25a, b) with Eq. (16) for $\theta_{wc} = 1$ & $\varepsilon_w \to 0$ yields

$$\frac{Nu_x}{Re_x^{0.5}\,Pr_c^{1/3}} = 0.331 \tag{29}$$

$$\frac{Nu}{Re^{0.5}Pr_c^{1/3}} = 0.662 \tag{30}$$

The two above results are the known exact ones of forced convection. Here, it is to state that exact solutions (27) to (30) confirm the proposed model validity.

3.2 Numerical solution

The theoretical model described by the nonlinear Eqs. (20) - (23) has to be solved simultaneously to find the *X*-distribution of the unknown parameters Δ_f, Δ_{tc}, θ_{wf} and θ_{wc} for certain values of conjugation parameters λ and ε_w. At first, Eqs. (22) & (23) are solved together to determine the *X*-distribution of Δ_{tc} and Δ_f for certain values of λ and ε_w Then, the corresponding distributions of θ_{wf} & θ_{wc} can be calculated from Eqs. (20) & (21), respectively. The numerical procedure starts at $X = 0$ for $\Delta_f = 0$ and $\Delta_{tc} = 0$, and then moves with small ΔX to arrive the point of $X = 1$. In the initial solution trails, exact results (27) to (30) were used as a benchmark to define the proper size of ΔX, which gives correct and stable results. It was found that the solution with $\Delta X = 0.004$ yields accurate and reliable results. The fourth-order Runge-Kutta tool was employed to perform this numerical task.

Figures 2-4 display numerical results found for zero wall resistance case of $\varepsilon_w = 0$. In this situation, the wall acts as a solid-fluid interface separating the two-fluid media. Figure 2 shows the variation in the local wall temperature θ_w at X=0.5 with λ-variable. It rises with decreasing λ to take finally the value 1 of the saturation temperature of the vapour side as $\lambda \to 0$. While it decreases with increasing λ to assume finally the value zero of the free-stream temperature of the convection side as $\lambda \to \infty$. The local conjugate Nusselt number, Nu_x at the same point of X=0.5 is plotted versus λ-variable in Fig. 3. Nu_x enhances with increasing λ and vice versa. It approaches the Nusselt result (27) of film condensation on isothermal vertical surfaces when $\lambda \to \infty$, while approaches the exact result (29) of forced convection on isothermal plan surfaces as $\lambda \to 0$. This means that the thermal effectiveness of film condensation dominates with increasing λ, while that of the forced convection dominates with decreasing λ. This behavior is consistent with the physical meaning of λ – parameter given by Eq. (19). The effect of λ-parameter on the condensation-side temperature gradient at the wall θ'_{wf} and that of the convection side θ'_{wc} is displayed in Fig. 4; for $\varepsilon_w = 0$. θ'_{wf} increases while θ'_{wc} decreases with increasing

Some results displaying the effect of wall resistance factor ε_w in more details are presented in Figs. (5) & (6). The dependence of the two fluid temperature gradients at the wall sides θ'_{wf}, θ'_{wc} on the wall resistance parameter $\boldsymbol{\varepsilon_w}$ is plotted in Fig. 5; for $\lambda = 1$. The plot shows that both θ'_{wf}, θ'_{wc} reduce while the temperature drop across the solid wall ($\theta_{wf} - \theta_{wc}$) increases with increasing ε_w. The effect of ε_w on the wall temperature drop ($\theta_{wf} - \theta_{wc}$) is more evident displayed in Fig. 6. It is noted that the temperature drop ($\theta_{wf} - \theta_{wc}$) rises with increasing ε_w, while decreases with increasing X. These results plotted in Figs. (5) & (6) indicate that the solid wall acts as a thermal obstacle between the film condensation and forced convection, which relaxes their thermal interaction. The variation in the mean conjugate Nusselt number, Nu, with λ and ε_w parameters is plotted in Fig. 7. The top curve of $\varepsilon_w = 0$ is limited by the two lines of the exact solutions (28) & (30) of film condensation and forced convection, respectively, on isothermal vertical plane surfaces. The plot shows that mean Nusselt number, Nu improves with rising λ-parameter, while reduces with increasing ε_w-parameter. Around 3000 numerical data points of mean conjugate Nusselt number, Nu could be correlated within ±2% (cf., Fig. 8) by:

$$\frac{Nu}{Ra_f^{.25}} = \left[0.9352 + \frac{0.1295}{(1+\lambda)^{.55}} - \frac{1.0537}{(1+\lambda)^{1.1}}\right] \frac{1}{(1+0.45\varepsilon_w^{0.9}/\lambda^{0.54})}; \qquad \text{for } 0.0 \le \varepsilon_w \le 0.5 \;\&\; 0.02 \le \lambda \le 30 \qquad (31)$$

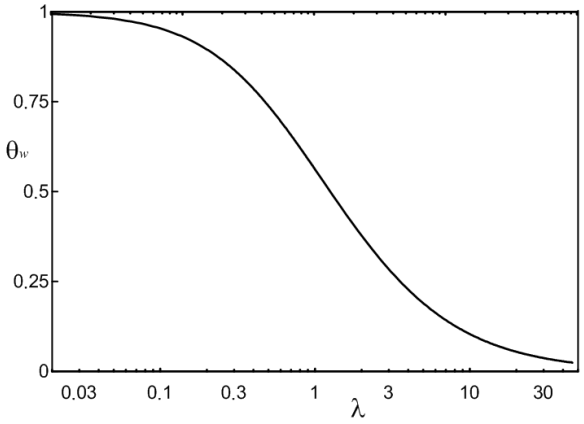

Fig. 2. Variation of wall temperature θ_w at X=0.5 with λ-; for ε_w = 0.

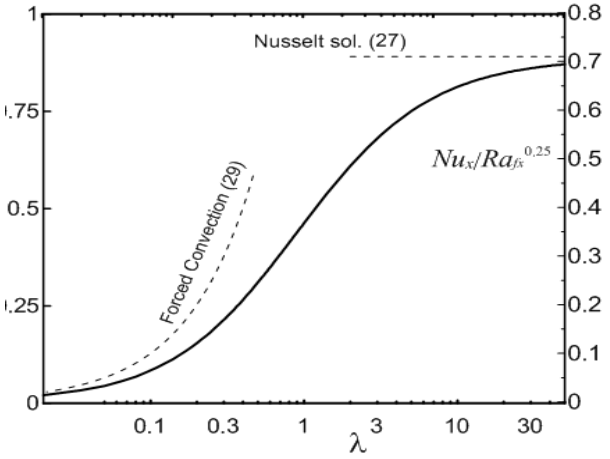

Fig. 3. Variation of local conjugate Nusselt number with λ; for X=0.5 & ε_w = 0.

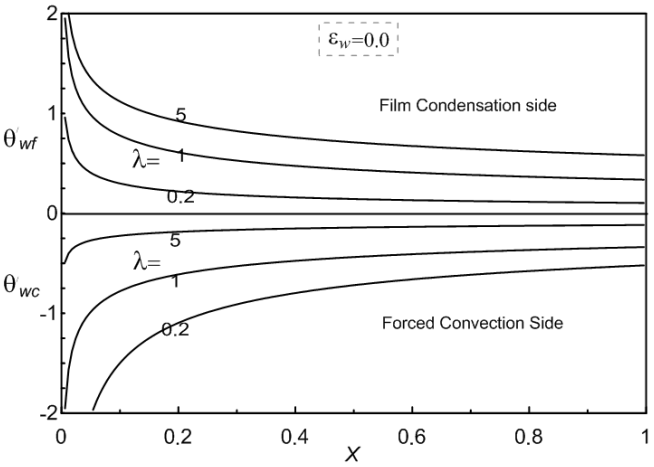

Fig. 4 Effect of λ on fluid temperature gradients at wall sides θ'_{wf} & θ'_{wc}; for ε_w=0.

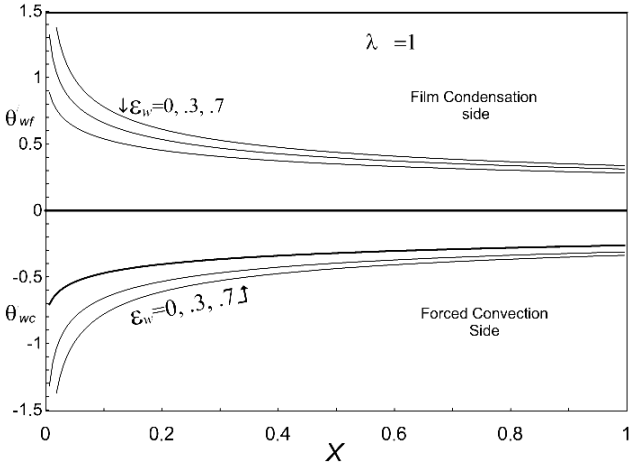

Fig. 5. Dependence of fluid temperature gradients at wall sides θ'_{wf} & θ'_{wc} on ε_w.

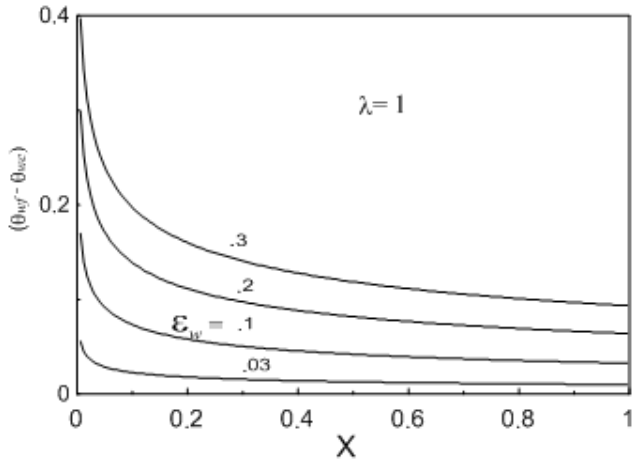

Fig. 6. Distribution of temperature drop across wall for different ε_w -parameter.

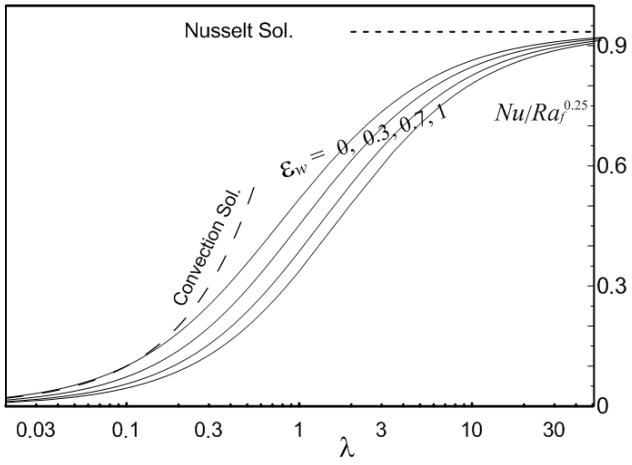

Fig. 7. Variation of mean conjugate Nusselt number with λ and ε_w parameters.

3.3 Model validation

It is indicated in subsection 3.1 that for zero wall resistance case of $\varepsilon_w = 0$, the model yields analytically the same known exact results (27)-(30) of laminar film condensation and forced convection on isothermal vertical surfaces. This proves our model validity. However, for the considerable wall resistance case of $\varepsilon_w > 0$, unfortunately, no practical or theoretical data (to our knowledge) are available in the literatures to be used for comparing with to test the model validity in this ε_w range. An alternative way is to construct special model problems, which can also be solved numerically by employing the known Fluent program. Then, a comparison between Fluent and model solutions can be made. For this objective, a model problem was constructed referring to Fig. 1. In this problem, the solid wall is a 1-mm, stainless steel sheet of height, H = 0.5 m and thermal conductivity k =16 W/ (m ^{o}C.). The vapour medium is a pure saturated steam of T_{s} = 100 ^{o}C. The cooling fluid is a pure water of free-stream velocity $u_{c\infty,}$ = 0.7 m/s and temperature $T_{c\infty}$ = 30 ^{o}C. The Fluent software (V. 14.5) was used to solve this problem under the same simplifications applied in the present model. For these problem data, the corresponding values of λ and $\varepsilon_{w,}$ calculated by Eq. (19), are 1.253 and 0.058, respectively. These λ and ε_w values are used to calculate our model solution. A comparison between model and corresponding Fluent results is displayed in Fig. 9, which shows an agreement of ± 3%. Some recent condensers are made from composite-polymer solid plates of low thermal conductivity to avoid high cost and corrosion [18-20]. Therefore, the same special problem was resolved for an identical composite-polymer plate of thermal conductivity k = 2.5 W/ (m K) instead the stainless-steel plate. In this case, the calculated values of λ and ε_w are 1.253 and .347, respectively. A comparable agreement between the present model and Fluent results was also found. However, this comparison is not displayed in a graph to avoid repetition.

As a brief report on the Fluent procedure applied, the mass, momentum and energy boundary-layer equations of forced convection and condensate film were solved together with the wall conduction equation using a control-volume scheme. A second-order upwind scheme was used to linearize the energy and momentum equations. A segregated solver was used to solve the resultant linear equation system. Under-relaxation factors were introduced to control the solution convergence. Rectangular cells with successive ratio = 1.03 were used in both fluid domains, while square cells were chosen for the wall region. As a convergence measure to stop the solution trails, the variation in all temperature and velocity nodes was set to be $\leq 10^{-6}$.

4. Conclusions

A theoretical model has been constructed for the conjugate problem of film condensation on the vertical surface of a solid wall cooled on the back side by forced flow. The forced-convection boundary layer was analyzed by employing the integral technique, and the film condensation by employing the boundary layer theory and Nusselt-Rohsenow simplifications. The study indicated that the conjugation between film condensation and forced convection across a conductive solid wall is governed mainly by two dimensionless factors λ and ε_w. The factor λ represents the ratio of condensate film to forced convection layer resistance, while the dimensionless factor ε_w represents the ratio of solid wall to forced convection layer resistance. For the special case of negligible wall resistance, the model yields analytically the same known exact results of film condensation and forced convection on isothermal vertical surfaces. This proves the model validity. The model was also solved numerically by employing the Runge-Kutta procedure for the parameter ranges: $0 \leq \varepsilon_w < 0.7 \;\&\; 0.01 < \lambda < 40.$ Numerical results showed that the mean conjugate Nusselt number rises with increasing λ or/and decreasing ε_w . An explicit simple formula for predicting the mean conjugate *Nu*

number as a function of λ and ε_w could be obtained by correlating around 3000 numerical data points within ±2 %. The model validity has also been tested by a comparison with Fluent results.

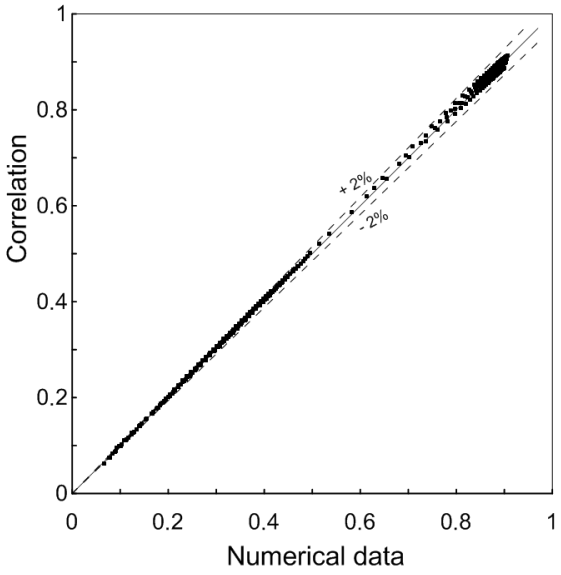

Fig. 8. Correlation (31) against correlated data.

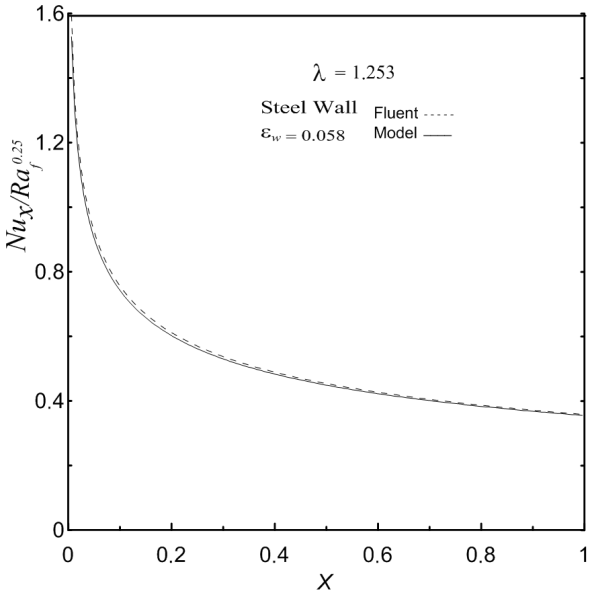

Fig. 9. Comparison between model and Fluent results.

Acknowledgements

This work supported and funded by The Public Authority For Applied Education and Training of Kuwait. Research Project No (TS-16-08), Research Title (Heat transfer characteristics of coupled film condensation and forced flow).

Nomenclature

g	gravitational acceleration, [m.s^{-2}]
l_f	scale of condensate film thickness, cf. Eq. (4), [–]
H	wall height, [m]
h_{fg}	latent heat, [J/kg]
Ja	Jacob number, = $C_{p_f}(T_s - T_{c\infty})/h_{fg}$, [–]
k	thermal conductivity, [W/(m ^{o}C)]
Nu	mean conjugate Nusselt number, [–]
Nu_x	local conjugate Nusselt number, [–]
Pr	Prandtl number, = ν/α, [–]
Ra_f	modified Rayleigh number of condensate film, cf. Eq. (4), [–]
Ra_x	local Rayleigh number of condensate film, Eq. (4), [–]
Re	Reynolds number of cooling fluid, = $u_{c\infty}H/\nu_c$, [–]
T	temperature, ^{o}C
$T_{c\infty}$	bulk temperature of cold forced-flow side, ^{o}C
T_s	vapour saturation temperature, ^{o}C
$u_{c\infty}$	free velocity of cold-side fluid, [m.s^{-1}]
u v	dimensional velocity components, [m.s^{-1}]

U, V	dimensionless velocity components
$x,\ y$	dimensional vertical and horizontal coordinates
X,Y	dimensionless vertical and horizontal coordinates

Greek letters

Δ_f	dimensionless thickness of condensate film
Δ_{tc}	dimensional thickness of thermal convection boundary layer
α	thermal diffusivity, [–]
ν	kinematic viscosity, [–]
λ	thermal resistance ratio of condensate film to forced convection layer
θ	dimensionless temperature
θ_{wc}	dimensionless temperature at wall side facing convection forced flow
θ_{wf}	dimensionless temperature at wall side facing condensate film
$\theta'_f(X,0)$	dimensionless temperature gradient of condensate film at wall
$\theta'_c(X,0)$	dimensionless temperature gradient of convection layer at wall
ε_w	thermal resistance ratio of wall to forced convection boundary layer
ρ	density, [kg.m^{-3}]

Subscripts

c	convection
f	condensate film
v	vapour
w	wall

References

[1] Nusselt, W., Die Oberflachen Kondensation des Wasserdampes, Z. Ver. Deut. Ing., 60(1916), pp.541–546

[2] Winkler, C.M., Chen, T.S., Minkowycz, W.J., Film condensation of saturated and superheated vapors along isothermal vertical surfaces in mixed convection, Numerical Heat Transfer, 36(1999), pp. 375–393

[3] Rohsenow, W.M., Heat transfer and temperature distribution in laminar film condensation," Trans. ASME, J. Heat Transfer, 78(1956), pp. 1645–1648

[4] Xu, H., You, X. Ch., Pop, I., Analytical approximation for laminar film condensation of saturated stream on an isothermal vertical plate, Appl. Math. Model, 32(2008), pp. 738-748

[5] Chang, T.-B., Mixed-convection film condensation along outside surface of vertical tube in saturated vapor with forced flow, Applied Thermal Engineering, 28 (2008), pp. 547–555

[6] Le, Q.T., Ormiston, S.J., Soliman, H.M., A closed-form solution for laminar film condensation from quiescent pure vapour on curved vertical walls, Int. J. of Heat and Mass Transfer, 73(2014), pp. 834–838

[7] Kim, S., Lee, Y.-G., Jerng, D.-W., Laminar film condensation of saturated vapor on an isothermal vertical cylinder, Int. J. of Heat and Mass Transfer, 83(2015), pp. 545–55

[8] Poulikakos, D., Interaction between film condensation on one side of a vertical wall and natural convection on the other side, J. of Heat Transfer, 108(1986), pp. 560-566

[9] Char, M.-H., Lin, J.-D., Conjugate film condensation and natural convection between two porous media separated by a vertical wall, Acta Mechanica, 148(2001), pp. 1-15

[10] Mosaad, M., Natural convection in a porous medium coupled across an impermeable vertical wall with film condensation, Heat and Mass Transfer, 22(1999), pp. 23-30
[11] Rashed Al-Ajmi, M. Mosaad, Heat exchange between film condensation and porous natural convection across a vertical wall, FDMP, 8(2011), 1, pp.51-67
[12] Patankar, S. V., Sparrow, E. M., Condensation on an extended surface, J. of Heat Transfer, 101(1979), pp. 434– 440
[13] Faghri, M., Sparrow, E.M., Parallel flow and counter flow on an internally cooled tube, Int. J. Heat Mass Transfer, 23 (1980), pp. 559-56.
[14] Kose, S., Theoretical investigation of Conjugate condensation heat transfer inside vertical tubes, Doctor Thesis, Middle East Technical University, Turkey, 2010
[15] Chen, H.T., Chang, S.M., Thermal interaction between laminar film condensation and forced convection along a conducting wall, Acta Mechanica, 118(1996), pp. 13 -26
[16] Bautista, O., Méndez, F., Treviño, C., Graetz problem for the conjugated conduction-film condensation process, Thermophysics and Heat Transfer, 14(2000), pp. 96-102
[17] Luna, N., Méndez, F., Film condensation process controlled by a Darcy cooling fluid flow, Thermophysics and Heat Transfer, 18(2004), pp. 388-394
[18] C. Heinle and D. Drummer, "Potential of thermally conductive polymers for the cooling of mechatronic parts," Physics Procedia, 3(2010), pp. 735-744.
[19] J. G. Cevallos, A. E. Bergles, A. Bar-Cohen, P. Rodgers and S. K. Gupta, "Polymer Heat Exchangers- History, Opportunities, and Challenges," Heat Transfer Engineering, 12(2012), pp. 1075-1093
[20] R. Trojanowski, T. Butcher, M. Worek, G. Wei, Polymer Heat Exchanger Design for Condensing Boiler Applications. Applied Thermal Engineering, 103(2016), PP. 150-158